

Retraction

Retracted: Tiny Spherical Robot with a Magnetic Field-Based Interference Detection and Prevention Framework

Advances in Materials Science and Engineering

Received 20 June 2023; Accepted 20 June 2023; Published 21 June 2023

Copyright © 2023 Advances in Materials Science and Engineering. This is an open access article distributed under the Creative Commons Attribution License, which permits unrestricted use, distribution, and reproduction in any medium, provided the original work is properly cited.

This article has been retracted by Hindawi following an investigation undertaken by the publisher [1]. This investigation has uncovered evidence of one or more of the following indicators of systematic manipulation of the publication process:

- (1) Discrepancies in scope
- (2) Discrepancies in the description of the research reported
- (3) Discrepancies between the availability of data and the research described
- (4) Inappropriate citations
- (5) Incoherent, meaningless and/or irrelevant content included in the article
- (6) Peer-review manipulation

The presence of these indicators undermines our confidence in the integrity of the article's content and we cannot, therefore, vouch for its reliability. Please note that this notice is intended solely to alert readers that the content of this article is unreliable. We have not investigated whether authors were aware of or involved in the systematic manipulation of the publication process.

Wiley and Hindawi regrets that the usual quality checks did not identify these issues before publication and have since put additional measures in place to safeguard research integrity.

We wish to credit our own Research Integrity and Research Publishing teams and anonymous and named external researchers and research integrity experts for contributing to this investigation.



The corresponding author, as the representative of all authors, has been given the opportunity to register their agreement or disagreement to this retraction. We have kept a record of any response received.

References

- [1] M. R. A. Refaai, S. Meenatchi, B. Ramesh, N. I. H. Rashid, N. B. Soni, and M. Ganesan, "Tiny Spherical Robot with a Magnetic Field-Based Interference Detection and Prevention Framework," *Advances in Materials Science and Engineering*, vol. 2022, Article ID 3908975, 10 pages, 2022.

Research Article

Tiny Spherical Robot with a Magnetic Field-Based Interference Detection and Prevention Framework

Mohamad Reda A. Refaai ¹, S. Meenatchi,² B. Ramesh,³ N. I. Haroon Rashid,⁴ N. B. Soni,⁵ and Manikandan Ganesan ⁶

¹Department of Mechanical Engineering, College of Engineering in Al-Kharj, Prince Sattam bin Abdulaziz University, Al-Kharj 11942, Saudi Arabia

²Department of Computer Science and Engineering, Institute Vellore of Technology (VIT), Vellore 632007, Tamil Nadu, India

³Department of Mechanical Engineering, Mohamed Sathak Engineering College, Kilakarai 623806, Tamil Nadu, India

⁴Department of Aerospace Engineering, B.S.A.R. Crescent Institute of Science and Technology, Vandalur, Chennai, Tamilnadu, India

⁵Department of Electrical Engineering, University of Petroleum and Energy Studies, Dehradun, Uttarakhand 248007, India

⁶Department of Electromechanical Engineering, Faculty of Manufacturing, Institute of Technology, Hawassa University, Hawassa, Ethiopia

Correspondence should be addressed to Manikandan Ganesan; mani301090@hu.edu.et

Received 6 May 2022; Revised 3 July 2022; Accepted 25 July 2022; Published 25 September 2022

Academic Editor: K. Raja

Copyright © 2022 Mohamad Reda A. Refaai et al. This is an open access article distributed under the Creative Commons Attribution License, which permits unrestricted use, distribution, and reproduction in any medium, provided the original work is properly cited.

Spherical robots are a recent technique and have attracted attention due to their capacity to move at high speeds while maintaining great locomotion efficiency. Many research studies have been undertaken on spherical robots' driving mechanisms, motion planning, and trajectory tracking systems, but only a few studies have been completed on their obstacle avoidance capacity. Its interfering prevention method was "hit and run" due to the existence of a sealed outer shell. This is convenient because of the spherical robots' unique shape. It might cause major problems when the robots are light and small in size. A high-speed collision with a hard surface might harm the robot or the camera in portable spherical robots with onboard cameras. In this article, a magnetic field-based interference detection and prevention system for a tiny spherical robot has been established. The proximity sensor uses a passive magnetic field to detect ferromagnetic barriers by causing the magnetic field to be perturbed. It makes use of a passive magnetic field to keep the system small and power-effective. Because the suggested system can sense not only the existence of a ferromagnetic barrier but also its approaching direction, an intelligent avoidance behaviour may be developed by combining the detection information with the trajectory tracking technique. It amplifies the disturbance effectively and hence increases the detection performance. To improve obstacle detection performance, design optimization is carried out and specific avoidance techniques are designed.

1. Introduction

Autonomous mobile robots have attracted a lot of interest in the robotics field during the last few decades and issues connected to their navigation have inspired a lot of research. Nonholonomic robots, being one of the most advanced types, offer a broad range of uses in surveillance and transportation. Depending on the application environment,

several locomotion techniques have been used [1]. Spherical robots have remained an extensive research and development area owing to their natural geometry and effective mobility technology. All of the working components of a spherical robot are wrapped inside the spherical shell and insulated from possible exterior risks or intrusion, making them ideal for release missions, reconnaissance, and even submerged operations [2]. Due to the many benefits

depending on the unique shape and locomotion mechanism, spherical robots have been an attractive research area for decades. All of the components and control units are wrapped inside, making it a closed system. As a result, they are safe from potentially dangerous surroundings. Rolling is a very efficient locomotion strategy that allows the battery to be smaller and the total robot control mechanism to be smaller [3]. Homeland security, rescue missions, and underwater operations are just a few of the possible uses. One of the most often touted benefits of spherical robots is their ability to recover quickly and naturally after colliding with objects. It avoids becoming trapped, unlike multilegged robots that merely roll back when they hit an item. This is tolerable for well-built robots, but it is an issue for small-sized robots, which often have a flimsy, fragile shell to reduce weight.

VIRGO is a new small spherical robot created by the Singapore University of Technology and Design (SUTD) that has exceptional observation abilities and a long battery life. The powertrain is made up of a discrepancy drive cart unit that works on the same principle as a hypocyclic gear train. Because of its simplicity and miniaturization possibilities, this drive mechanism was chosen. It has been consistently worked on to increase its dynamic performance while reducing its total size [4].

Figure 1 shows that small spherical robots have a lightweight thin plastic outer shell that allows them to achieve linear motion at high speed but only provides a modest shield from impacts. When such robotic platforms are utilized for monitoring, the situation gets even worse. Because these robots are carrying sensitive payloads such as cameras, high-impact accidents should be avoided rather than permitted in these applications. As a result, a proximity-detecting system with no contact must be included in order to provide remedial navigation signals [6]. The onboard sensor hardware and processes must be sensibly planned and established due to the limited space and processing power. Mobile robot navigation is commonly divided into three categories: trajectory tracking, motion planning, and obstacle avoidance. Approaches for planning global motion, such as potential field approaches and sampling planners, have been thoroughly investigated [7]. The algorithms used for scientific analysis of defined geometry need previous knowledge of the operating space and impediments. For the centralized planning to construct a distributed robotic structure while considering the size limitation and low compute capabilities, VIRGO has been sought. A pure-pursuit controller controls VIRGO's trajectory tracking and point-to-point locomotion. The twist of the continuing path, which ends at the target waypoint and starts at the robot's present location, is computed using the pure-pursuit algorithm [5].

The accuracy of waypoint tracking has been shown. The obvious benefit of a spherical robot, in terms of obstacle avoidance, has been highlighted repeatedly; its capacity to rebound from accidents has been highlighted as well. Because of this, there is little research on obstacle avoidance for spherical robots. Obstacle avoidance capability is required for decentralized yet small spherical robots such as VIRGO



FIGURE 1: Spherical robot (VIRGO) [5].

not only to increase navigation effectiveness but also to enhance the robot's endurance without surrendering its weight [8]. Closed construction becomes a challenge when building a proximity sensor for spherical robots. Many typical obstacle detection technologies, such as ultrasonic sensors, need a clear line-of-sight. If the shell is translucent, infrared or laser might pass through it. However, after conducting practical tests with the infrared sensor, the scientists discovered that the performance had deteriorated owing to scratching between the shell and the ground, which produces signal diffraction and refraction. The transmission of electromagnetic-based sensing is unaffected by the plastic shell, making it more promising [9]. One of the most important aspects of autonomous navigation for mobile robots is real-time obstacle detection and avoidance. Collision avoidance is built into all autonomous robots, ranging from simple algorithms that identify an impediment and direct the robot to avoid collisions to complex algorithms. Urban obstacles, such as walls and furniture, may have metal components that cause an electromagnetic field disruption. Capacitive coupling, induction coupling, and static magnetic field disorder are some of the interactions that cause it.

In this article, a magnetic field-based interference recognition and prevention system for a tiny spherical robot has been established. The proximity sensor uses a passive magnetic field to detect ferromagnetic barriers by causing the magnetic field to be perturbed. It makes use of a passive magnetic field to keep the system small and power-effective. Because the suggested system can sense not only the existence of a ferromagnetic barrier but also its approaching direction, an intelligent avoidance behaviour may be developed by combining the detection information with the trajectory tracking technique. It amplifies the disturbance effectively and hence increases the detection performance. To improve obstacle detection performance, design optimization is carried out and specific avoidance techniques are designed.

2. Related Work

Inverse perspective mapping (IMP) is focused on estimating the geometric cues in detecting obstacles. At the IPM stage, a vertical plane model is used to boost performance. The IPM data and the acquired floor appearance model are then used

to perform appearance-based obstacle segmentation. The shortest distance between the robots and the avoided interference is then determined. The suggested technique was tested on 70 datasets, including nonobstacle photos with significant floor appearance variations. The accuracy of quantitative segmentation is then associated with a standard approach, which has constructed and also estimated the distance accuracy of the proposed system [10]. The oscillating magnetic field localization technology is demonstrated, which is a compact and highly precise proximity sensing structure. The main issue in RF-based social distance sensing techniques is overcome using the sense modality, which is based on an oscillating magnetic field with a low frequency, which is a reliable notion that disables the main issue of RF-based social distance sensing methods in terms of dependability. Because the magnetic field intensity created by coils is proportional to distance, creating magnetic fields for inside scenarios such as rooms, hallways, or factories often necessitates powerful motionless sources with coils and high inductance. The oscillating object with a smaller magnetic field system is appropriate for wearable applications, which produce enough radius for the variety of social isolation. This method effectively produces a tiny magnetic field “bubble” around the travelling user to establish a social distancing zone for them. As a result, social distance breaches may be detected without the need to know the specific location of the user [11].

A full vision-based motion control system for magnetic microrobots has been developed to solve the challenge of controlling them. Even in a congested environment with barriers such as bubbles or impurities, high-resolution impurity detection may be accomplished. A strategic and functional strategy is provided for recognizing and mapping these impediments in the environment in real time, as well as designing optimum barrier-free mobility paths to arrive at the goal point in the shortest time possible. By self-modifying the intended course, the magnetic microrobot can design a trajectory in a fluid environment. The control is generally regulated to within 10 microns of precision [12]. It has varied strong external magnetic fields, allowing a systematic characterisation of the performance of commercial off-the-shelf UAV motors. Two distinct motor types (Air Gear and SwellPro) are explored, as well as two different control systems (direct torque control and field-oriented control). The research study does not include a review of more complex control methods [13]. As an industrial surveillance robot, a spherical robot design and its applications are presented. This robot is meant to act as a human’s extended eye, inspecting the state of the pipe system or other areas that are difficult to inspect owing to their placement. The robot used in this study is semiautonomous, meaning that it is controlled by a human using an android user interface. By looking at the display, the user may operate the robot. This study discusses the input analysis of how the signal can move the robot. The proposed method’s usefulness has been demonstrated in an experimental setting in a comparable scenario [14].

The UWB indoor positioning of multiple sensor fusion has many methods for improving accuracy with high-coast

proven optimal. Because of its low cost, UWB positioning technology can attain centimetre-level precision in a two-dimensional plane, but its accuracy in a three-dimensional space is still developing. Furthermore, little research has been carried out on the problem of significant interference between UWB signals, i.e., irregular data fluctuations induced by time delay would result in an erroneous indoor location. As a result, precise placement of UWB amid signal interference (e.g., obscuration between anchors and target) is seen as a pressing issue that must be addressed. A UWB indoor high-precision positioning model based on GA-optimized ELM is proposed, with a binary classifier based on GA-ELM to judge the presence of signal interference and positioning error compensation using the GA-ELM model to realise the precise positioning of the mobile robot target in complex indoor environments [15]. To tackle the issues, techniques for machine learning are presented. According to reports, using the k-nearest neighbour technique (k-NN) is a machine-learning technique to obtain decent results based on the accuracy of localization and computing speed. Furthermore, it has been claimed that using artificial neural networks (ANNs) rather than using k-NN can increase localization accuracy even further [16].

A unique way of overcoming obstacles is using touch sensors on each of the robot’s legs. Leg positioning is usually indicated by touch sensors on the feet of legged robots. In our example, the robot had touch sensors on the front side of each leg that alerted it to the presence of an impediment in front of each leg. It can also be utilized as a backup input in the event that the robot’s vision-based system fails. Finally, the tactile obstacle avoidance approach may be used with additional environmental recognition sensors to provide the best possible identification of the robot’s surroundings. In comparison to visual systems that need processing time, this approach allows for reactive responses to barriers and is practically immediate. Tactile sensors can also be employed in low-light or no-light situations, where a computer vision-based solution would be ineffective [17].

By reducing the posteriori covariance under the Kalman gain constraint, an optimum partial-state updating Kalman filter (PS-EKF) is suggested. It isolates the magnetic disturbance from two level angles and the sensors’ biases. The PS-EKF may be simply integrated with the magnetic disturbance detecting approach based on thresholds. The classic threshold-based technique identifies magnetic disturbances by imposing a limit on the magnetic norm, the angle between gravity and the measured magnetic field, or both. Because the observed magnetic direction and the reference magnetic field cannot be totally restricted in the same direction, these approaches may lead to defect discovery. In this regard, a vectorial magnetic disturbance detection technique is suggested, which compares the calculated measurement’s norm and direction directly with the reference magnetic field [18]. The decision field theory (DFT) is used to introduce the perception of the decision-making force. DFT is a psychologically based dynamic-cognitive method for human decision making that was first described as a deterministic-dynamic model of a method based on the avoidance of conflict behaviour. When the robot comes

across an impediment, the decision-making force will determine which way is best to avoid the obstruction. A closed-loop control system, dynamic disgust field, and decision force are combined to create an obstacle avoidance algorithm. It recognises that the robot follows a continuous motion trajectory rather than a specific goal point, that the robot can return to its original motion trajectory after avoiding obstacles, and that the decision-making force gives a parametric solution rather than a single prevention choice [19].

3. Materials and Methods

3.1. Spherical Robot Modelling. Another form of mobile robot whose motion is provided by an inner pendulum mechanism is the spherical robot. The benefit of this robot is that its motion is rolling, and because all of the mechanical parts are contained within the sphere, it may be used in a marine or wet environment. The actuator on this robot is coupled to a perpendicular axis which is shown in Figure 2 [20].

To balance robot motion, the spherical robot arrangement has two actuators and two counterweights. The inner elements are structured in such a way that the center's mass is aligned with its geometrical center. The robot's center of mass is connected to its gravity and has an impact on its dynamics.

3.2. Dynamic Modelling. The torque and force applied, as well as the influence of torque and force on robot motion and energy created, are all affected by dynamics modelling in spherical robots [21]. The study of the robot's path planning and control necessitates the use of dynamics. This is given in Figure 3.

The dynamic modelling in spherical robots has the effect of torque and force on the robot's motion and energy generated. The acceleration robot is achieved by equations (1)–(4).

$$x'' = -2d(p_0''p_2 - p_1''p_3 - p_2''p_0 + p_3''p_1), \quad (1)$$

$$y'' = d(p_0''p_0 - p_1''p_0 + p_2''p_2 + p_3''p_3), \quad (2)$$

$$\|p'\|^2 + p_0''p_0 + p_1''p_0 + p_2''p_2 + p_3''p_3 = 0. \quad (3)$$

The complete position $p = [x, y, p_0, p_1, p_2, p_3, \varnothing_x, \varnothing_y, \varnothing_z]^T$ and the applied torque is $\tau = [0, 0, 0, 0, 0, \tau_x, \tau_y, \tau_z, 0]^T$, the dynamics of the special robot are given as follows:

$$M(p)p' + v(p, p') + G(p) = \tau. \quad (4)$$

The angular distance is $\theta_x, \theta_y, \theta_z$, where p -state variable, $M(p)$ -total mass, $v(p, p')$ -centrifugal force, $G(p)$ -gravitational force, and τ -torque.

3.3. Proximity Sensor for the Passive Magnetic Field

3.3.1. Design Concept and Modelling. The Earth's magnetic field is used in existing research to identify magnetic

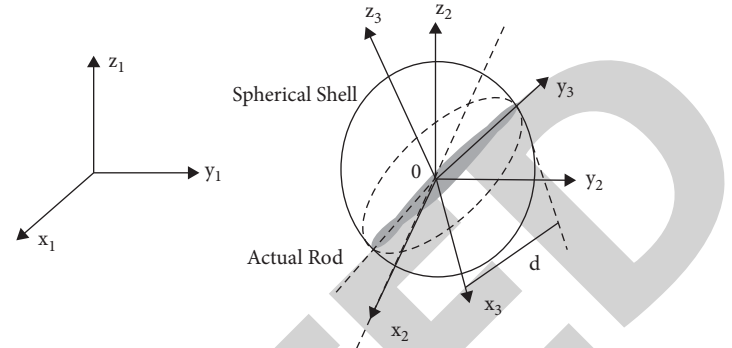


FIGURE 2: A spherical robot with an actuator.

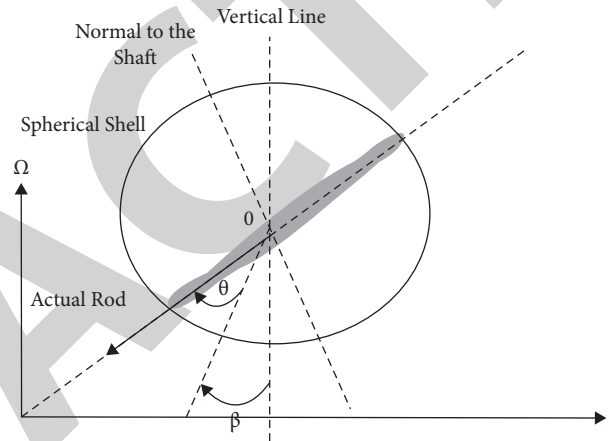


FIGURE 3: Rolling motion of a spherical robot.

abnormalities. The Earth's magnetic field on the ground may be assumed to be unchanging and parallel to the ground by modelling the Earth as a large dipole magnet, which is employed in the present research to find magnetic irregularities. This field has no external source and distorts everywhere a ferromagnetic material is present [22].

The signal-to-noise ratio can be accompanied due to the signal strength and disturbance field, which is one of the major hurdles in putting this method to practical use. The distortion caused by the object is considerably less compared to the steel object. Furthermore, the distortion is directional, with the direction determined by both the Earth's magnetic field and the geometry of the ferromagnetic item. Simulating the distortion field when just the Earth's magnetic field is present can be difficult. The strength of the magnetic field on Earth is in the range of 25 to 65 μT .

While the object's substance and size are proportional to the amplitude of the field of distortion and it can be regularized, the magnetic location of the object in reference to the geomagnetic field is unknown until its direction varies from location to location in the geomagnetic field. Many strategies have been applied to amplify and extract information from the tiny distortion field. To get a useable signal, several of them gave up on the directional capability. A sensor construction with a particularly constructed passive magnetic field to magnify the alteration field is proposed here.

Due to the distinct and distinctive field design, it is feasible to calculate the magnetic location of this item. This feature will also allow for direction prediction, which is required for the robotic planning path. The fundamental concept is to produce a magnetic field with a high spatial gradient by strategically arranging two permanent magnets. When a ferromagnetic object is present, the magnetic field is disturbed. A magnetic field sensor with low power may detect an instantaneous field distortion since the magnetic fluxes are constant. This distortion field is significantly stronger when the Earth's magnetic field occurs.

3.3.2. Principles of Detection Based on a Magnetic Field.

When the Earth is modelled as a massive dipole magnet, the magnetic field on the ground should be homogeneous and parallel to the ground. When a ferromagnetic item is present, this field, which has no external source, gets distorted.

It is significantly tougher to detect slight deviations in a weak field, which is represented in Figure 4. It is problematic to describe the perturbation field caused by a nearby ferromagnetic object when just the Earth's magnetic field is occurring. The field in this scenario is determined not only by the object's composition and form but also by its magnetic direction in relation to the geomagnetic field. Materials and forms can be normalized since they have a proportionate relationship with the amplitude of the perturbation field. The magnetic orientation in relation to the geomagnetic field is uncertain, owing to the fact that the geomagnetic field direction varies from different places. Many approaches have been investigated to extract location information from minor field fluctuations. To obtain a large enough signal, several of them compromised the direction-detecting function. However, for interference avoidance and path planning in robotic applications, direction detection is critical. As a result, a specifically constructed passive magnetic field is used to increase the perturbation field while simultaneously detecting the orientation of a nearby item.

3.3.3. Design Approach and Theoretical Analysis.

A magnetic flux loop with a balance system is constructed by the judicious positioning of two permanent magnets, inspired by the electrical Wheatstone bridge, and allows minor resistance variations to be sensed. The main concept is to produce a magnetic field with a high spatial gradient artificially. As a result, if a ferromagnetic item is present, the magnetic field will be disrupted. The instantaneous field fluctuation generated by this interruption will be significant since the magnetic fluxes are incessant and have strong spatial gradients.

The magnetic flux lines are focused towards the sensor due to the occurrence of the ferromagnetic plate and its greater permeability than that of air. Because the magnetic flux loop is incessant and has a significant spatial gradient, even a minor item might create significant problems. As a result, when the suggested design is employed as a proximity sensor, the magnetic flux density response is improved and detected by the magnetometer. Because of the one-of-a-kind nature of this interaction, knowing the spatial pose of the

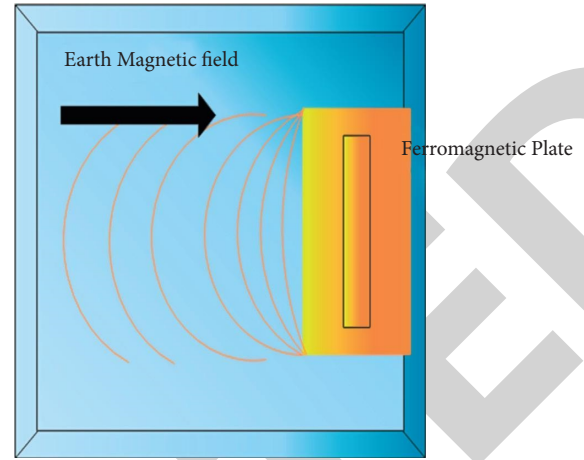


FIGURE 4: Distortion due to a ferromagnetic plate.

item that creates the disturbance will necessitate a theoretical explanation of the magnetic field perturbation.

The material, approaching angle, object size, and distance between the magnets and the object would all influence the magnetic field distortion created by the item. To make the analysis easier, the material penetrability is expected to be infinite and the size of the object is considered to be substantially large. The magnetic field analytical 2D system is built using the imaging technique and the magnetic charge design due to the interface between the permanent magnet.

The magnet surface is parallel to the x axis while the magnetization axis is parallel to the z axis. The magnetic charge model uses the product of the surface normal vector and the magnetization to compute negative and positive surface charges. The magnetic field is calculated by mixing the surface charge influence with respect to the pole region. In this case, magnetic charges of comparable strength and the opposite sign are used to substitute the material barrier to account for the magnetic consequence exerted by the object.

The impending direction of the item is parallel to the x axis for simplicity of demonstration of the picture technique. In real-world situations, it is more likely that the items will approach at an angle rather than parallel. The picture magnetic charges' placement is determined by the impending angle and the distance between the magnets and the impediment. Furthermore, the positioning of the coordinate system is affected by the approaching angle. The variation in the magnetic field based on the image is given as in equation (5).

$$\Delta B = B_i = T \times \frac{\mu_0}{4\pi} \left(\oint \frac{-\sigma_i (L_s - L_i)}{|L_s - L_i|^3} ds - \oint \frac{\sigma_i (L_s - L_i)}{|L_s - L_i|^3} ds \right), \quad (5)$$

where $T = \begin{bmatrix} \cos 2\alpha & -\sin 2\alpha & 0 \\ \sin 2\alpha & \cos 2\alpha & 0 \\ 0 & 0 & 1 \end{bmatrix}$, T-transformation matrix,

σ_i -magnetic charge in the image, L_s -location of the field,

L_i -location of the image, and s - surface area of the magnet image.

3.3.4. Design Integration and Optimization. The configuration of VIRGO is analyzed initially in order to match the spherical robot and the magnetic proximity sensor. All of the working components of VIRGO, including the controller, camera, DC motors, and battery, are housed in a framework in the sphere's middle section. The motion is transferred to the shell via two wheels positioned at the bottom of the chassis [23].

The permanent magnets with opposite magnetism may be put on the moving framework facing top and bottom, allowing the robot to be seamlessly integrated with minimal reconfiguration.

When the cameras were pointed forward and the diameter of the magnet was limited, square-shaped magnets were chosen over disk-shaped magnets to maximize the area. The present IMU contains a built-in magnetometer that can be utilized for this type of sensing. An additional magnetometer is utilized here to investigate the interference detection and robot motion performance distinctly.

The magnitude of the distortion field is presented due to an approaching obstacle and is given by the following equation:

$$|\Delta B| = \frac{\mu_0 \sigma_i |L_s|}{4\pi} \left(\oint \frac{1}{|L_s - L_i|^3} ds - \oint \frac{1}{|L_s - L_i|^3} ds \right), \quad (6)$$

where L_s -location of the sensor and L_i -location of the image.

The optimization problem is formed by maximizing the magnitude of distortion as shown in the following equation:

$$(V, \gamma, W) = \operatorname{argmax} \left(\sum_{L=L_1, L_2, \dots, L_n} |\Delta B| |L| \right), \quad (7)$$

where $L = L_1, L_2, \dots, L_n$ -magnetic field location

As the distance to the interference rises, the magnitude decreases, as illustrated by equation (7). Due to the infinite assumptions on the magnetic permeability of the barrier and the obstacle height, equation (6) cannot be utilized to precisely forecast the quantity of distortion field in real life. The magnetic field distortion is expected to occur on a smaller scale and within a smaller area of finite objects with limited magnetic permeability.

The variation in the normalized field is given as in the following equation:

$$\frac{\Delta B}{|\Delta B|} = \frac{L_s}{|L_s|} - \begin{bmatrix} \cos \alpha \\ \sin \alpha \\ 0 \end{bmatrix}, \quad (8)$$

where L_s -location of the arbitrary field.

When $R_s = [0 \ 0 \ 0]^T$, then the angle of the normalized field is given as in the following equation:

$$\alpha = \arctan \left(\frac{\Delta B_y}{\Delta B_x} \right). \quad (9)$$

The difference field due to a ferromagnet will point near the object's position when the sensor is situated at the precise middle point between the two magnets, according to equation (9). Although the above derivations are based on the premise that the item is indefinitely huge and has infinite permeability, the result holds for finite objects. Furthermore, most barriers for tiny spherical robots will be much larger than the robot itself.

3.3.5. Obstacle Detection and Avoidance. The obstacle detecting system's mechanical incorporation and configuration optimization have been examined [24]. The approach of a ferromagnetic barrier can be detected by monitoring magnetic field data continuously and analyzing the disruption. A prediction system on a moving platform, unlike a single sensor on the ground, must continually inform the reference field to separate the distortion field formed by an approaching item from noise readings caused by shifting positions. A moving-window average of measurements is generated on a continual basis, with the most recent findings serving as the reference field. The robot controller estimates the distance between its present location and the specified waypoint when a target waypoint is given. If the distance is within the look-ahead distance limit, the pure-pursuit controller generates a trajectory using the distance and the robot heading. As a consequence, the wheel speed could be accurately adjusted. If the distance is less than the minimum look-ahead distance, the trajectory is constructed using the least look-ahead distance. To prevent the robot from attempting to reach an unreachable location, the look-ahead distance is set to double the robot's radius.

Calibrated data are generated by deducting this reference data from each new measurement, which is then utilized for interference detection, which is given in Figure 5.

For trajectory tracking, the VIRGO platform currently employs a pure-pursuit algorithm [25]. The tuning coefficient is employed to adjust the robot's mobility behaviour. The robot chooses to go in a broad arc when the destination waypoint is on the side; when the value is tiny, the robot chooses to walk in a twisting manner. The green lines below show how the executed trajectory is made up of several arcs. To avoid an increase in motion deviation, the robot controller calculates the curves repeatedly.

When the control unit detects an impediment, an interruptive process is initiated, which comprises discontinuing the motor, rotating on the plug, and proceeding to the intermediate waypoint. After retrieving the preceding waypoint, the trajectory will be recalculated using the current position as the starting point. If the robot's speed exceeds the constancy threshold, causing it to topple if it comes to a rapid halt, the robot will first slow down before coming to a complete stop. When the robot identifies the impediment, the control unit will make this choice based on the predefined constancy threshold and the speed of the robot.

Figure 6 illustrates the algorithm for the detailed description of the controller and sensor mechanism in a spherical robot. The obstacle avoidance flag is set when the sensor data achievement thread analyses the data. Based on

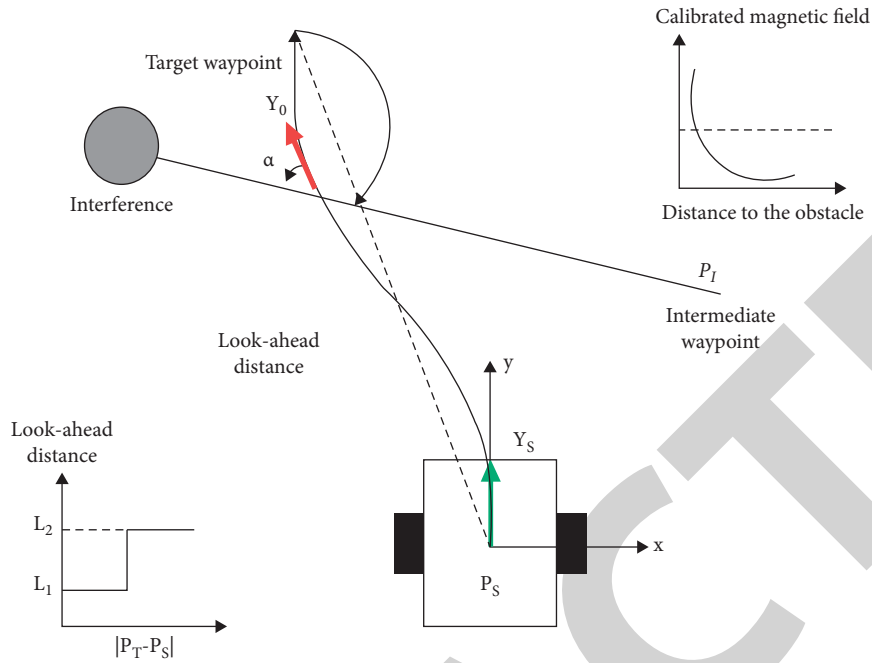


FIGURE 5: Interference avoidance behavior of integration.

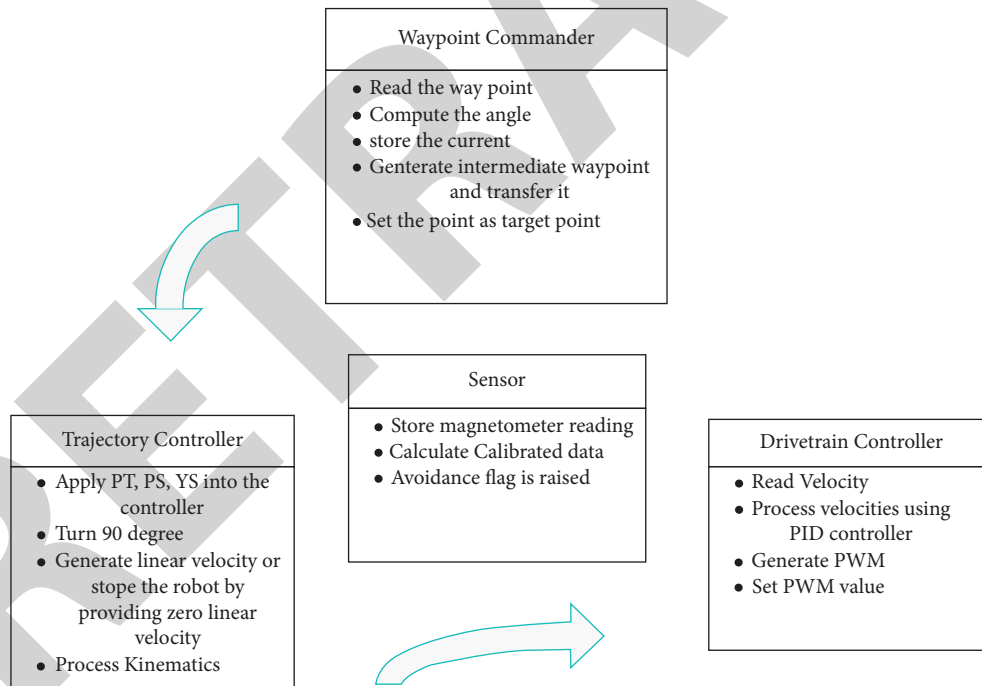


FIGURE 6: Representation of a detailed algorithm.

the interference avoidance flag, the commander of the waypoint creates the target waypoint from a set of choices. The velocities are calculated by the trajectory controller from the desired waypoint based on the interference prevention flag. Finally, the drivetrain controller uses the anticipated wheel velocities to regulate the motor. Although some variables are shared between threads, such as the destination waypoint, interference prevention flag, and velocities, the execution of all four threads is not in any specific order. They

all begin and end at the same time but with different loop frequencies.

3.3.6. *Obstacle Prevention.* Interference can be avoided by using a range of magnetic field sensors such as ultrasonic, laser, and infrared sensors. The accuracy of the proposed system is improved by using range estimation. The unknown interference can be detected simultaneously with the robot

to evade collision and move towards the destination. The interference detection can be examined by the following aspects.

- (1) Determining the obstacles that has the proximity of the spherical robot
- (2) The projection of the obstacles as given in the following equation:

$$p_k = \operatorname{argmin} \|x - p\|. \quad (10)$$

- (3) p_k is the potential function based on the obstacle point

The obstacle can be avoided by using the potential field function. The range of interaction of a robot is given by the following equation:

$$N = k\epsilon V: \|p_k - p\|, \quad (11)$$

where $\|\cdot\|$ -Euclidean norm, p -position of robot, and p_k -position of obstacles.

The constrains of the spherical robot and the obstacles are represented by the following equation:

$$\|p_k - p\| = d, d < r. \quad (12)$$

The navigation of the obstacles can be achieved using the potential of the system as given in the following equation:

$$V(p) = c_1 V_o(p) + c_2 V_n(p), \quad (13)$$

where c_1, c_2 -positive constant and V_o, V_n - interactive potential.

$$V_n(p) = \sum \left(\sqrt{\left(1 + \|p - p_r\|^2\right)} - 1 \right), \quad (14)$$

where p_r -target position of spherical robot.

The collision avoidance is achieved using the energy function as given in the following equation:

$$H(p, q) = V(p) + T(p), \quad (15)$$

where $V(p)$ -potential energy and $T(p, q)$ -kinetic energy of the robot.

The condition $H' < 0$ shows that the collision never occurs between the spherical robot and obstacles.

4. Result and Discussion

Considering the configuration of the robot and its size, the design optimization strategies can be chosen and embedded on the robot system. The optical motion tracking system is used to evaluate the performance of the obstacle avoidance by capturing the behavior of the robot using the IR camera. Table 1 provides the parameters of the robot which are used to evaluate the performance of obstacle avoidance.

4.1. Calibration. An industrial robot is utilized to transfer a ferromagnetic material about the sensor to evaluate the practical sensor performance and standardize the accuracy of angle detection. The robot is positioned on a nonmagnetic

TABLE 1: Mechanical parameters of the robot.

IMU	Bosch BNO055
Magnetometer	MAG3110
Magnet	0.5-inch length and 0.125-inch height
Controller	STM32F411RE
Motor	Max RPM:119
Wheel	2 mm of width and 10 mm of diameter

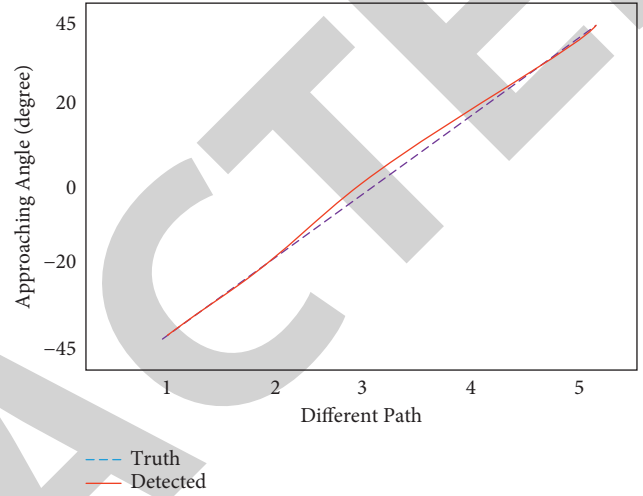


FIGURE 7: Accuracy of angle detection.

surface, and the robot's hand moves an 8 cm long steel cube. Between the two magnets, a MAG3110 three-axis magnetometer is attached, and data are collected using an Arduino Uno board. The object is directed at the robot from various angles in the frontal area and the impending angle of the object can be estimated from the magnetic field. The average value for each approaching angle is estimated with an object at a different distance, which is shown in Figure 7.

Table 2 examines the errors such as average detection error and maximum detection error. The error is estimated based on the variation in the detected angle, which is analyzed using an error bar with an average value due to the estimation with different distances.

Figure 8 shows the magnitude of the distortion field measured. When the object is nearer to the magnetometer, maximum distortion is detected. The magnitude of the distortion field reduces as the distance increases. The trends in approaching angle are shown by the relationship between the distance and magnitude of the object.

4.2. Effect of Distance Separation. When the distance between the two magnets is greater, the magnet's volume has a greater effect on the performance of object detection. The influence of separation distance among the two magnets, as well as magnet geometries, is utilized here. The volume is the same but with different aspect ratios. When the barrier is positioned at a succession of incremental locations, a summation of the magnitude of the distortion fields is determined.

TABLE 2: Approaching angle detected based on the designed angle.

Intended angle	-45	-30	0	30	45
Predicted angle	-45.8	-19.2	1.9	21.6	46.3
Typical error (%)	1.8	1.6	2.3	2.7	1.3
Increase error detection	3.2	2.5	3.4	2.8	2.2
Maximum error (%)	3.5	2.6	3.3	3.5	2.6

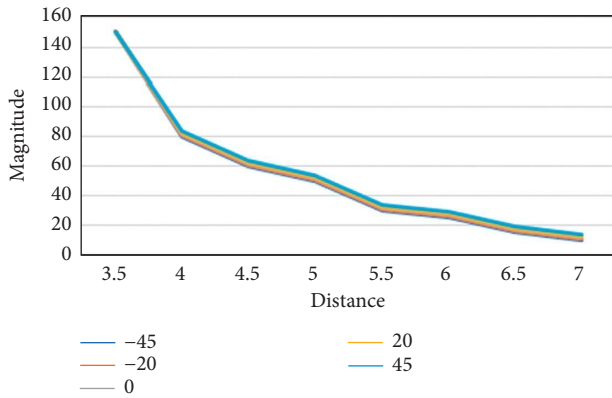


FIGURE 8: Comparison between the magnitude and distance of the robot to the ferromagnetic object.

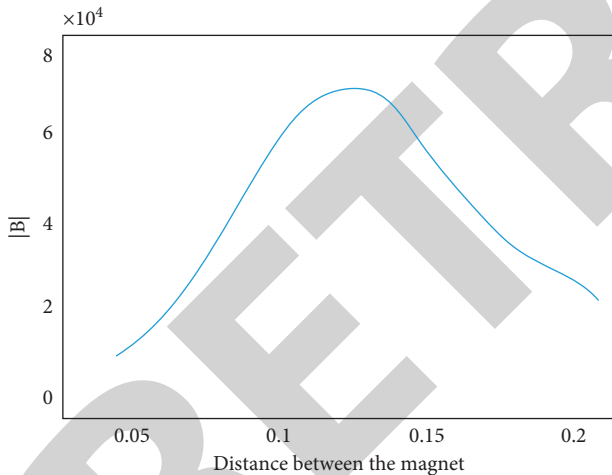


FIGURE 9: Effect on distortion field strength due to the distance separation between two magnets.

Figure 9 shows that the distortion field magnitude increases with the distance and when the magnets are separated for more distance, it reaches its maximum value.

Figure 10 shows this distortion field based on the effect of the magnetic field. In spite of the distance between the two magnets, the amplitude of the distortion field grows significantly with the magnet volume. Despite the fact that the aspect ratio of these two magnets differs from that of the previous three magnets, the influence of the aspect ratio reduces the distance between the two magnets.

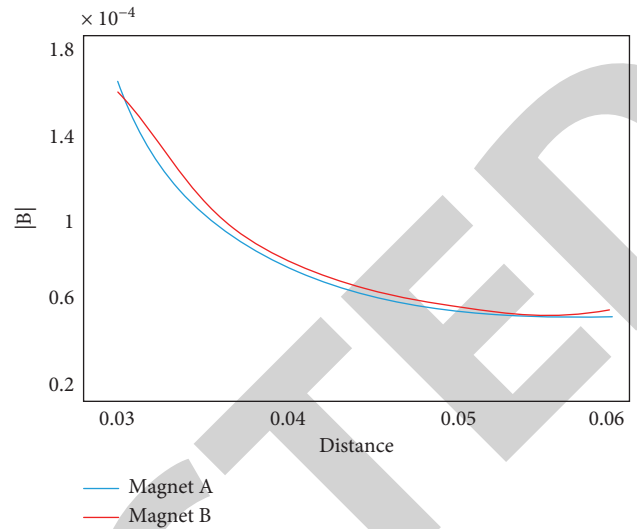


FIGURE 10: Effect of magnet geometry on distortion.

5. Conclusion

In this paper, a VIRGO microspherical robot with a proximity sensor for a passive magnetic field was developed and obstacle avoidance behaviour was realised.

- (i) It has been established that the enhanced robot can evade physical contact with impediments while still reaching its intended destination waypoint. The robot does not need to be reconfigured in order to use this innovative sensing technology, and the dimensions of this tiny spherical robot do not change.
- (ii) Not only can the sensing system identify the existence of an adjacent ferromagnetic object but it can also offer essential information about the direction of an object approaching, which is crucial for course planning and interference prevention.
- (iii) The robot may use this information to calculate and execute correction orders in real time to prevent colliding and causing damage. To increase the system’s sensing accuracy, further studies will involve optimization on the sensor design and an automatic calibration machine. The small sensing system will eventually be incorporated with a collision avoidance algorithm into the spherical robot platform.

Data Availability

The data used to support the findings of this study are included within the article. Further data or information are available from the corresponding author upon request.

Conflicts of Interest

The authors declare that there are no conflicts of interest.

Acknowledgments

The authors appreciate the support from the Hawassa University, Ethiopia, for the research and preparation of the manuscript. The authors thank the Vellore Institute of Technology and the B.S.A.R. Crescent Institute of Science and Technology for providing assistance with this work.

References

- [1] Y. Zhu, B. Jin, Y. Wu, T. Guo, and X. Zhao, "Trajectory correction and locomotion analysis of a hexapod walking robot with semi-round rigid feet," *Sensors*, vol. 16, no. 9, p. 1392, 2016.
- [2] S. Pan, L. Shi, and S. Guo, "A Kinect-based real-time compressive tracking prototype system for amphibious spherical robots," *Sensors*, vol. 15, no. 4, pp. 8232–8252, 2015.
- [3] I. A. Taha and H. M. Marhoon, "Implementation of controlled robot for fire detection and extinguish to closed areas based on Arduino," *TELKOMNIKA*, vol. 16, no. 2, p. 654, 2018.
- [4] A. R. Chowdhury, G. S. Soh, S. Foong, and K. L. Wood, "Implementation of caterpillar inspired rolling gait and nonlinear control strategy in a spherical robot," *Journal of Bionic Engineering*, vol. 15, no. 2, pp. 313–328, 2018.
- [5] V. A. Ajay, A. P. Suherlan, G. S. Soh, S. Foong, K. Wood, and K. Otto, "Localization and trajectory tracking of an autonomous spherical rolling robot using imu and odometry," in *Proceedings of the Volume 5A: 39th Mechanisms and Robotics Conference*, vol. 57120, Article ID V05AT08A058, France, Europe, 2015.
- [6] A. A. Kilin, E. N. Pivovarova, and T. B. Ivanova, "Spherical robot of combined type: dynamics and control," *Regular & Chaotic Dynamics*, vol. 20, no. 6, pp. 716–728, 2015.
- [7] D. Lau, J. Eden, and D. Oetomo, "Fluid motion planner for nonholonomic 3-D mobile robots with kinematic constraints," *IEEE Transactions on Robotics*, vol. 31, no. 6, pp. 1537–1547, 2015.
- [8] H. Xing, S. Liwei, and Y. He, "Hybrid locomotion evaluation for a novel amphibious spherical robot," *Applied Sciences*, vol. 8, no. 2, p. 156, 2018.
- [9] M. Bujňák, R. Pirnik, K. Rastocny et al., "Spherical robots for special purposes: a review on current possibilities," *Sensors*, vol. 22, no. 4, p. 1413, 2022.
- [10] T.-J. Lee, D.-H. Yi, and D.-I. Cho, "A monocular vision sensor-based obstacle detection algorithm for autonomous robots," *Sensors*, vol. 16, no. 3, p. 311, 2016.
- [11] S. Bian, B. Zhou, and P. Lukowicz, "Social distance monitor with a wearable magnetic field proximity sensor," *Sensors*, vol. 20, no. 18, p. 5101, 2020.
- [12] X. Tang, Y. Li, X. Liu, D. Liu, Z. Chen, and T. Arai, "Vision-based automated control of magnetic microrobots," *Micro-machines*, vol. 13, no. 2, p. 337, 2022.
- [13] M. Heggo, A. Mohammed, J. Melecio et al., "The operation of UAV propulsion motors in the presence of high external magnetic fields," *Robotics*, vol. 10, no. 2, p. 79, 2021.
- [14] T. Dewi, P. Risma, Y. Oktarina, and R. Kusumanto, "Motion control analysis of a spherical robot as a surveillance robot," *Journal of Physics: Conference Series*, vol. 1167, Article ID 012004, 2019.
- [15] J. Ma, X. Duan, C. Shang, M. Ma, and D. Zhang, "Improved extreme learning machine based UWB positioning for mobile robots with signal interference," *Machines*, vol. 10, no. 3, p. 218, 2022.
- [16] A. i. Sasaki, "Effectiveness of artificial neural networks for solving inverse problems in magnetic field-based localization," *Sensors*, vol. 22, no. 6, p. 2240, 2022.
- [17] M. Luneckas, T. Luneckas, D. Udris, D. Plonis, R. Maskeliūnas, and R. Damaševičius, "A hybrid tactile sensor-based obstacle overcoming method for hexapod walking robots," *Intel Serv Robotics*, vol. 14, no. 1, pp. 9–24, 2021.
- [18] M. Zhu, W. Ouyang, and Y. Wu, "Orientation estimation by partial-state updating kalman filter and vectorial magnetic interference detection," *IEEE Transactions on Aerospace and Electronic Systems*, vol. 57, no. 3, pp. 1815–1826, 2021.
- [19] W. Zhang, H. Cheng, L. Hao, X. Li, M. Liu, and X. Gao, "An obstacle avoidance algorithm for robot manipulators based on decision-making force," *Robotics and Computer-Integrated Manufacturing*, vol. 71, Article ID 102114, 2021.
- [20] H. Ghariblu and H. Mohammadi, "Structure and dynamic modelling of a spherical robot," in *Proceedings of the 2012 8th International Symposium on Mechatronics and its Applications*, pp. 1–5, Sharjah, UAE, April 2012.
- [21] V. Muralidharan and A. D. Mahindrakar, "Geometric controllability and stabilization of spherical robot dynamics," *IEEE Transactions on Automatic Control*, vol. 60, no. 10, pp. 2762–2767, 2015.
- [22] B. George, H. Zangl, T. Bretterkieber, and G. Brasseur, "A combined inductive-capacitive proximity sensor for seat occupancy detection," *IEEE Transactions on Instrumentation and Measurement*, vol. 59, no. 5, pp. 1463–1470, 2010.
- [23] Y. Ye, C. Zhang, C. He, X. Wang, J. Huang, and J. Deng, "A review on applications of capacitive displacement sensing for capacitive proximity sensor," *IEEE Access*, vol. 8, Article ID 45325, 2020.
- [24] A. Discant, A. Rogozan, C. Rusu, and A. Bensrhair, "Sensors for obstacle detection-a survey," in *Proceedings of the 2007 30th International Spring Seminar on Electronics Technology (ISSE)*, pp. 100–105, Cluj-Napoca, Romania, May 2007.
- [25] B. Song, J. Luo, R. E. Mohan, and K. L. Wood, "Data-driven function network analysis for product platform planning: a case study of spherical rolling robots," in *Proceedings of the International Design Engineering Technical Conferences and Computers and Information in Engineering Conference*, vol. 51845, Article ID V007T06A040, Quebec, Canada, August 2018.